Journal of Physical Chemistry C

ARTICLE *in* THE JOURNAL OF PHYSICAL CHEMISTRY C · JANUARY 2015

Impact Factor: 4.77 · DOI: 10.1021/jp512144g

THE JOURNAL OF PHYSICAL CHEMISTRY C

Article

pubs.acs.org/JPCC

Structure of Mixed Self-Assembled Monolayers on Gold Nanoparticles at Three Different Arrangements

Vasumathi Velachi,*[,†] Debdip Bhandary,[‡] Jayant K. Singh,[‡] and M. Natália D. S. Cordeiro*[,†]

[†]REQUIMTE/Department of Chemistry and Biochemistry, Faculty of Sciences, University of Porto, 4169-007 Porto, Portugal

[‡]Department of Chemical Engineering, Indian Institute of Technology Kanpur, Kanpur, 208016, India

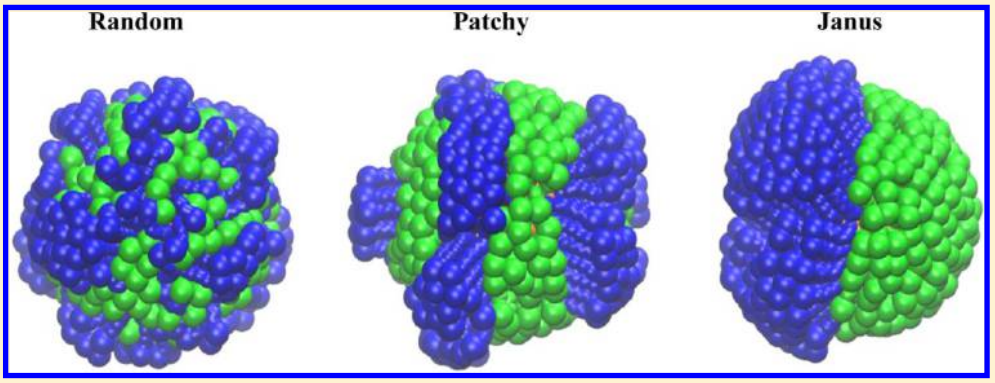

ABSTRACT: In this work, we performed atomistic simulations to study the structural properties of mixed self-assembled monolayers (SAM) of hydrophilic and hydrophobic alkylthiols, with two different chain lengths (C5 and C11), on gold nanoparticles (NPs) at three different arrangements, namely: random, patchy, and Janus domains. In particular, we report the effect of mixing of thiols with unequal carbon chain lengths (C5 and C11) at three different arrangements on the structural properties and hydration of SAMs. Our simulation study reveals that the arrangement of thiols having unequal carbon chains in mixed SAMs is a key parameter in deciding the hydrophilicity of the coated gold NPs. Thus, our findings suggest that the hydration of the SAMs-protected gold NPs is not only dependent on the molecular composition of the thiols, but also on the organization of their mixing. In addition, our results show that the bending of longer thiols, when these are mixed with shorter thiols, depends on the arrangement of thiols as well as the chemical nature of their terminal groups.

1. INTRODUCTION

Gold nanoparticles (AuNPs) coated with self-assembled monolayers (SAMs) of thiolates provide many unique features that make them attractive in multiple potential applications, including sensing, catalysis, drug delivery, electron transfer efficiency, electrochemical charging, and molecular recognition.[1−9] In fact, SAMs serve as a linker between the NPs and the environment, providing important properties to the material such as stability and solubility.[2,10,11] Therefore, understanding the structure of thiolate SAMs on AuNPs has been an active area of research. Many experimental groups have studied the structure of SAMs coated on nanoparticles using scanning tunneling microscopy (STM),[12−14] infrared spectroscopy (IR),[15] electron spin resonance (ESR),[16] mass spectroscopy,[17] transmission electron microscopy (TEM),[18] fluorescence,[19] and nuclear magnetic resonance (NMR).[20] Luedtke and Landman[21,22] were the first to report that the adsorption site geometries on nanocrystallites differ from those found on extended flat Au(111) and Au(100) surfaces, using molecular dynamics simulations. Later, Gorai et al.[23] studied the structural properties of SAMs ($SH—(CH_2)_n—CH_3$, n = 4−20) on AuNPs at low and high temperatures, and they conclude that the tilt angle depends strongly on the temperature and chain length of the alkanethiols. Recently, Lane et al.[24] reported that the terminal groups of the alkanethiols and the solvent play an important role in determining the properties of SAMs surface pattern on AuNPs.

SAMs predominantly determine the properties of the nanoparticles, as each type of alkanethiol in the mixed SAMs confers the NPs with a certain set of properties.[25] Hence, investigating the structural morphology of mixed SAMs coated on AuNPs is of great interest. The organization of mixed SAMs upon adsorption falls into two main categories, namely, completely mixed (random/stripe/patchy) and demixed (Janus) formation. Each organization is very important for the properties and functioning of the NPs. For instance, AuNPs with completely mixed arrangements lead to structure-dependent properties such as interfacial energy and solubility.[26,27] On the contrary, the demixed Janus particle-type arrangements can be used for assembling into unique structures.[28] Therefore, the investigation on SAMs of mixed thiols on gold NPs has attracted particular attention. Various experimental[12−20] and

Received: December 5, 2014
Revised: January 15, 2015
Published: January 16, 2015

DOI: 10.1021/jp512144g
J. Phys. Chem. C 2015, 119, 3199−3209

theoretical[29,30] studies have reported different kinds of mixed arrangements with the same and different carbon chain length of alkanethiols as well as mixture of aliphatic and aromatic thiols. Recently, Liu et al.[20] showed the possibility of three structural morphologies, namely, random, stripe/patchy, and Janus particles of mixed SAMs on gold NPs, using NMR.

In a recent paper,[31] we have studied and compared the structural properties of mixed SAMs on gold(111) surface at three different arrangements and inspect their surface hydrophilicity. We found that the surface hydrophilicity does not change much with different SAM arrangement, even though, thickness of SAMs varied a bit with different arrangement.[31] However, it is not clear how the SAMs get organized and hydrated in the case of mixed SAMs coated on curved surfaces (AuNPs) at three different arrangements. To the best of our knowledge, no previous simulation work has yet been carried out to address the above comparison study. Thus, with this motivation and as a continuation of our previous work, here we present a detailed simulation study of the structural properties of hydrophobic−hydrophilic mixed SAMs on AuNPs at three different arrangements, namely: random, patchy, and Janus. Recently, experimental and theoretical studies have shown that the structural properties of alkanethiols on AuNPs of a fixed size depend on the carbon chain length of thiols.[29,30] Therefore, in our study, we considered thiols with shorter (C5) and longer (C11) carbon chain lengths, as well as mixture of C5 and C11. The rest of the paper is organized as follows: in the next section we give details of the systems as well as of our molecular dynamics (MD) simulations; in section 3, we discuss the results from our MD simulations; finally, the main conclusions of this study are summarized in section 4.

2. SIMULATION DETAILS

The alkanethiols coated on AuNPs were modeled with an all atom representation. We built up icosahedral AuNPs with a diameter of 4 nm, containing 1985 Au atoms, using Material Studio 6.0. Although these icosahedral AuNPs have multiple faces such as (111) and (100), the overall structure looks almost spherical. Thus, the alkanethiols were grafted radially away from the NPs with a distance between the sulfur atoms of SAMs and the AuNPs surface of 2.38 Å. From our recent adsorption study, we found 370 thiols are adsorbed on AuNPs of 4 nm size which is quite reasonable number compared to 156 and 258 thiols for 2.4 and 3.2 nm in the previous adsorption study.[21,22] Hence, in the present work, 370 alkyl thiols were placed randomly on the AuNPs. Since AuNPs weakly interact with the alkanethiol coating and solvent, these were fixed during the simulations. In addition, since we aim to study the hydration and structural properties of SAMs at three different arrangements, we also fix the sulfur atoms. Four types of SAMs were considered for coating the AuNPs built, namely: (i) $S-(CH_2)_{11}-CH_3$ and $S-(CH_2)_{11}-COOH$, (ii) $S-(CH_2)_5-CH_3$ and $S-(CH_2)_5-COOH$, (iii) $S-(CH_2)_5-CH_3$ and $S-(CH_2)_{11}-COOH$, plus (iv) $S-(CH_2)_{11}-CH_3$ and $S-(CH_2)_5-COOH$, which hereafter will be denoted as C11−C11COOH, C5−C5COOH, C5−C11COOH, and C11−C5COOH, respectively. Further, for convenience, the random, patchy, and Janus type of arrangements will be called from now on as ran, pat, and Jan, respectively. Finally, all the coated AuNPs were placed at the center of a cubic box of dimensions of about 140 × 140 × 140 $Å^3$ and surrounded by a sufficient number of water molecules (ca. 67 100) to avoid the interactions between the SAMs and their periodic images. The periodic boundary conditions were applied in all Cartesian directions. The CHARMM27 force field[32] was used to describe the all-atom intermolecular interactions for SAMs, which has already been successfully applied in MD simulations of SAMs on gold surface in previous studies.[31,33−35] The Lennard−Jones (LJ) intermolecular potential was used to model the gold atoms[36] of NPs and the gold−sulfur interactions. The LJ cross-interaction parameters were calculated from the standard Lorentz−Berthelot[37] combining rules. Harmonic bond stretching, angle bending and dihedral angle terms were taken from the CHARMM27 force field.

All MD simulations were carried out using the LAMMPS package[38] on the isothermal−isobaric (NpT) ensemble with a time step of 1.0 fs. The temperature was kept constant at 298 K and the pressure at 1 atm by means of the Nosé−Hoover thermostat coupled with the Parrinello−Rahman barostat[39,40] with a relaxation constant of 0.1 ps. The Particle−Particle Particle-Mesh (PPPM) method[41] was used to handle the long-range electrostatic interactions with the real-space cutoff distance set to 12 Å and the error tolerance to 10^{-5}. The short-range LJ interactions were smoothly shifted to zero between 10 and 12 Å. The SHAKE algorithm[42] was used to constraints the bonds in water molecules. All the analyses presented in this paper were performed by averaging over the last 2 ns of the 4−5 ns NpT MD-trajectories, and the VMD software[43] was used for visualization of the trajectories and taking snapshots.

3. RESULTS AND DISCUSSION

3.1. Size of the SAMs-Coated AuNPs. We start our discussion with the size of the SAMs coated AuNPs formed in our simulations. We have analyzed the size of the SAMs coated AuNPs by calculating their radius of gyration (R_g) for all the cases, which are presented in Table 1. The obtained R_g values can provide a measure of the conformational changes of alkanethiols when these are adsorbed onto the AuNPs. In other words, for fixed AuNPs and thiol lengths, a lower R_g corresponds to larger tilting/bending of thiols and vice versa. From the results given in Table 1, it can be seen that only some changes in the average size of the SAMs coated on AuNPs at three different arrangements are observed for mixing of thiols with unequal carbon chain lengths. Particularly, patchy mixing has a slightly larger size when compared with the other kinds of mixed arrangements, indicating that its structural morphology is different from the others. This is due to the fact that, unlike flat coatings, NPs coatings (curvature coatings) of chains have free volume to explore even when they are densely packed at their grafting points (see Figure 1).[29,44,45] Thus, thiols segregate and self-assemble and maintains the terminal groups distance at ∼5 Å. In the case of random mixing, organization of the mixed thiols arises from an average orientation of thiols. Hence, thiols in random mixing segregate to form general clusters of

Table 1. Radius of Gyration for the AuNPs Coated with Mixed SAMs for All the Studied Cases

	ran	pat	Jan
C5−C5COOH	24.62 ± 0.78	24.66 ± 0.78	24.66 ± 0.78
C11−C11COOH	28.47 ± 0.90	28.50 ± 0.90	28.48 ± 0.90
C5−C11COOH	26.88 ± 0.85	27.02 ± 0.85	26.63 ± 0.84
C11−C5COOH	26.97 ± 0.85	27.24 ± 0.86	26.56 ± 0.84

DOI: 10.1021/jp512144g
J. Phys. Chem. C 2015, 119, 3199−3209

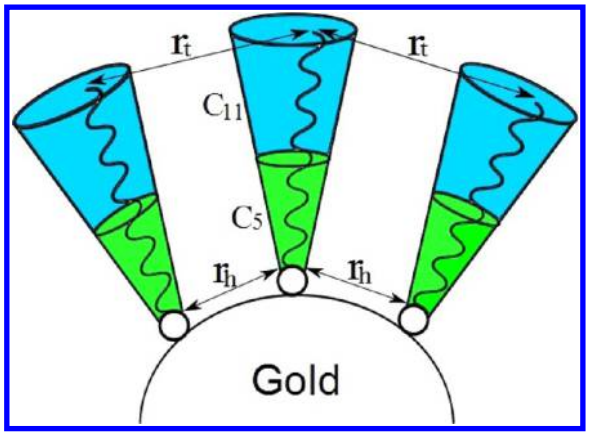

Figure 1. Schematic two-dimensional representation of the decreased density of thiols at increasing carbon chain length and the free volume available to the thiols. Green and cyan color cones refer to the free volume available for shorter and longer thiols, respectively. Here, $r_t > r_h$, r_h and r_t are the distance between the head groups and the tail groups, respectively.

hydrophobic and hydrophilic nature. As a result, longer thiols happened to tilt and bend more to fill the free space provided by the shorter thiols (see the discussion in the following sections), giving a more compact structure to C5−C11COOH and C11−C5COOH random arrangements. Whereas in the case of patchy mixing, the hydrophilic thiols segregate to form a small cluster that yields a distinct phase segregation of hydrophobic thiols. Due to this, the R_g values for C5−C11COOH and C11−C5COOH random mixing are somewhat smaller than that of the patchy mixing. The expected changes in geometric centers for both the C5−C11COOH and C11−C5COOH Janus mixing, due to the mixing of unequal carbon chain lengths, gives rise to lower R_g values even when compared with the corresponding random mixing. Therefore, in the case of unequal carbon chain length mixing of thiols, a direct comparison of the radius of gyration of Janus mixing with the other two kinds of mixing is not possible.

In order to understand the phase segregation of thiols, we have presented the equilibrated snapshots of all the cases in Figures 2 and 3. These snapshots give a more qualitative picture of adsorption of thiols on AuNPs, i.e., certain patterns are apparent in the images of the SAMs coated on AuNPs. For instance, in the case of C11−C11COOH mixing, patchy mixing shows distinct phase segregation for hydrophilic carboxyl termination, whereas hydrophobic methyl termination groups do not show such phase segregation. That is, the hydrophobic thiols are divided and then segregate a nearby hydrophilic cluster. Whereas in the case of random and Janus C11−C11COOH mixing, the SAMs segregate to large islands. However, C5−C5COOH mixing does not show any notable difference upon adsorption at three arrangements. Mixture of unequal carbon chain lengths of thiols shows interesting patterns. For example, patchy mixing shows formation of small clusters, random mixing shows more compaction pattern by bending of C11 thiols over C5 thiols, and Janus mixing shows an acorn nut like pattern. These interesting observations suggest that the SAMs get organized differently upon different mixing arrangements, particularly for C11−C11COOH patchy and unequal carbon chain length mixing, which can function differently.

3.2. Structure of SAMs. Generally, the structure of SAMs can be characterized mainly through their tilt angles, because

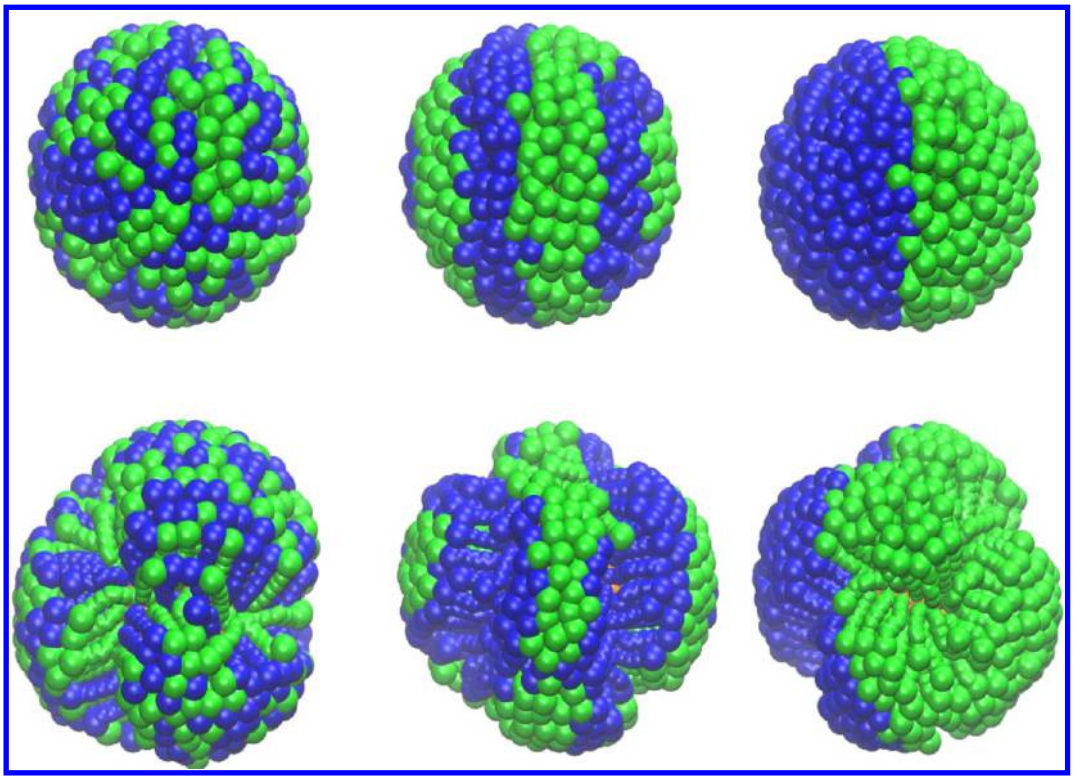

Figure 2. Equilibrated structures of the AuNPs coated with mixed SAMs of C5−C5COOH (top row) and C11−C11COOH (bottom row) at random, patchy and Janus arrangements (from left to right). Color coding: methyl terminated alkanethiols, blue; and carboxyl terminated alkanethiols, green.

DOI: 10.1021/jp512144g
J. Phys. Chem. C 2015, 119, 3199−3209

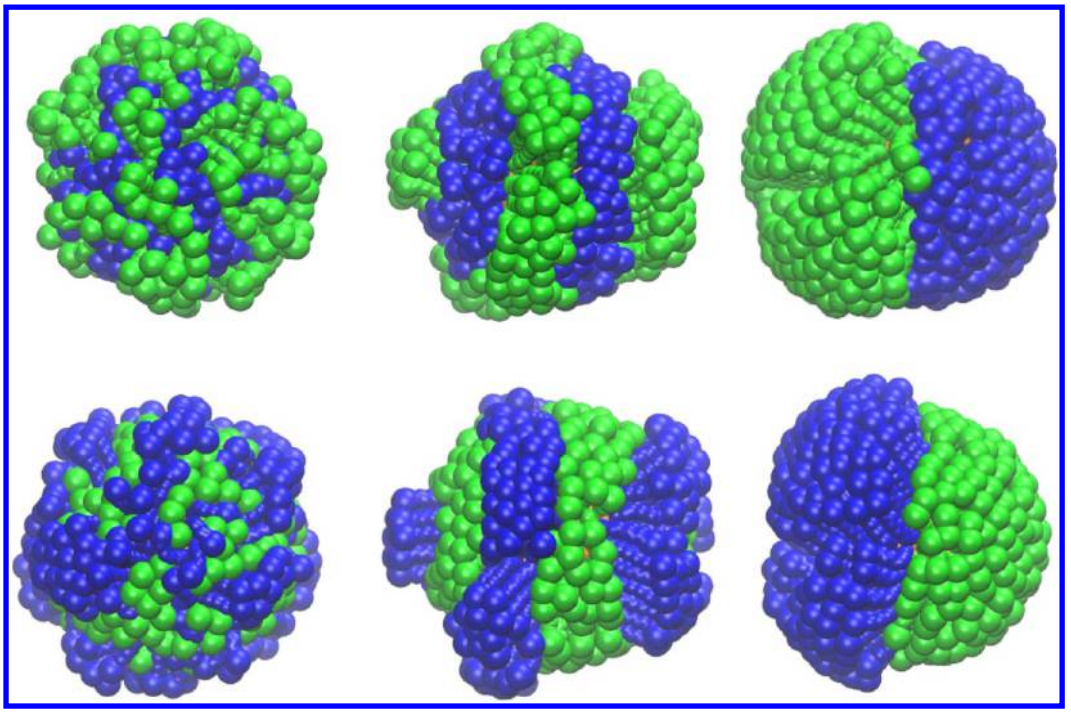

Figure 3. Equilibrated structures of the AuNPs coated with mixed SAMs of C5−C11COOH (top row) and C11−C5COOH (bottom row) at random, patchy and Janus arrangements (from left to right). Color-coding as in Figure 2.

Table 2. Average tilt angle of the mixed SAMs for all the studied cases

			C5−C11COOH		C11−C5COOH	
	C5−C5COOH	C11−C11COOH	CH_3 (C5)	COOH (C11)	CH_3 (C11)	COOH (C5)
ran	20 ± 11	31 ± 14	21 ± 11	33 ± 14	30 ± 14	21 ± 11
pat	21 ± 11	29 ± 13	22 ± 11	32 ± 13	27 ± 12	21 ± 12
Jan	21 ± 11	30 ± 13	21 ± 11	30 ± 13	31 ± 13	21 ± 12

alkanethiols are known to tilt when adsorbed onto a metal surface. Although there are several studies on the structure of tilted alkanethiol SAMs on flat gold surfaces,[46−49] such studies on the structure of tilted SAMs coated on AuNPs are scarce.[23,30] According to Gorai et al.,[23,30] the tilt angle of SAMs coated on AuNPs can be determined by finding the angle between the vector joining the sulfur headgroup and the odd carbons of the alkyl chain and the vector perpendicular to the surface of the sphere and passing through the sulfur headgroup. For a fixed NPs, the tilt angle increases by increasing the carbon chain length. The calculated tilt angles, summarized in Table 2, also reveal the same, i.e., the tilt angle for longer thiols (C11) is higher compared to the shorter thiols (C5). These tilt angle values are in good agreement with earlier computed results.[23,30] The average tilt angles for C5−C5COOH mixing are almost constant at three different arrangements. Alternatively, the tilt angle is slightly lower for the C11−C11COOH patchy mixing when compared to the other two arrangements. The reason for this lowering of tilt angle is due to the organization of thiols, that is, the patchy arrangement of thiols yields small clusters of phase segregation when compared to the Janus and random arrangements (see Figure 2). As a consequence of the curvature coating, the carbon chain density decreases by increasing the carbon chain lengths as it is schematically depicted in Figure 1.[29,44,45] Hence, longer thiols have more free volume available to tilt and we observed a smaller variation in the tilt angles for longer thiols mixing at three different arrangements compared to that seen for shorter thiols mixing. Previous computational studies[30] on AuNPs coated with mixed thiols with sufficient length variation showed that longer thiols tend to tilt more to fill the gap provided by the shorter thiols. Our results also suggest the same, but only for some cases. For example, in the case of C5−C11COOH mixing, random and patchy mixing shows more tilting compared with the equal length mixing case, whereas Janus mixing shows the same tilt angle as in the case of equal length mixing. However, in C11−C5COOH mixing, the tilting of longer thiols can be ordered as follows: Jan < ran < pat. As a result of the free volume provided by the longer carbon chain length of thiols, we observe variation in the tilt angles for different mixing arrangements. Adsorption of thiols on flat surfaces admits the inversely proportional relation between thickness and tilt angle, that is, the thickness increases or decreases as the tilt angle decreases or increases, respectively.[31,46−49] The behavior of tilt angles and R_g of SAMs coated AuNPs seen for NPs is akin to the behavior seen for the flat surfaces.

3.3. Bending of Thiols. Mixing of thiols with unequal carbon chain lengths provides the extra space for longer thiols by shorter thiols that not only allows longer thiols to adopt larger tilt angles, but it also may give a possible bending over the shorter thiols. Singh et al.[29] observed the bending of longer thiols over the shorter ones when their length substantially differs. To check the possibility of bending of longer thiols at three kinds of arrangements, we have calculated the end-to-end (C1 and C11 carbon) distance (R) which gives a qualitative

DOI: 10.1021/jp512144g
J. Phys. Chem. C 2015, 119, 3199−3209

measurement of the bending. Figure 4 shows the probability distributions of R/R_0, $P(R/R_0)$, where R is the end-to-end distance, i.e., the distance between the C1 and C11 carbon atoms, and R_0 is the geometric length of the carbon chain. In all cases, two distinct peaks are observed at $R/R_0 = 1$ and at $R/R_0 < 1$ corresponding to thiols without bending and with bending, respectively. The distribution shows a higher peak at $R/R_0 < 1$ for the C5−C11COOH randomly mixed SAM, clearly indicating bending of alkyl chains. In the other cases, though two peaks appear separately, the peak at $R/R_0 < 1$ is less probable. A higher value for the latter peak implies higher degree of bending and thus, we can state that the randomly mixed C5−C11COOH and C11−C5COOH SAMs show the maximum bending of alkyl chains among all the cases considered. That is, the random mixing of C5−C11COOH and C11−C5COOH gives more compact structures compared to the other two kinds of mixing, just as the sizes showed (see Table 1). In the case of random mixing, some of the longer thiols may not have longer thiols in their close vicinity for strong interactions and hence, the probability of bending of those is higher in this type of mixing. However, in the case of C5−C11COOH patchy mixing, even though the longer thiols will have one or two nearest neighbor thiols of similar kind for interactions, it shows higher bending probability than that of the C11−C5COOH patchy. The main reason here is that, due to the proximity of the three/four carboxyl terminal thiols, the terminal carboxyl groups have a greater possibility to make hydrogen bonds with water molecules than within themselves by bending slightly. This can be easily checked out by looking at the number of hydrogen bonds per carboxyl group with water molecules. From the end-to-end distance distributions, it is clear that, the longer thiols with carboxyl terminal groups are more intended to bend over onto shorter thiols than the longer thiols with methyl terminal groups. Further, the distributions clearly indicate that the adsorption of thiols at three different

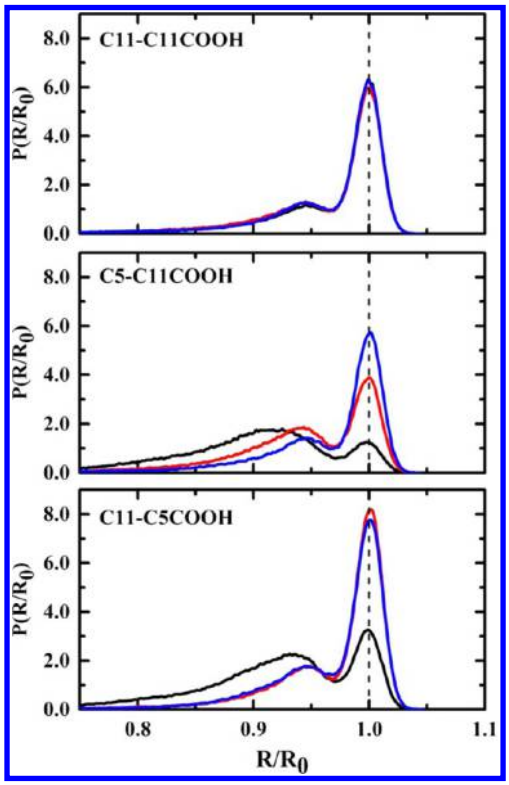

Figure 4. Probability distributions of the end (C1)-to-end (C11) distance for C11−C11COOH mixing, C5−C11COOH mixing and C11−C5COOH mixing at random (black color), patchy (red color), and Janus (blue color) arrangements.

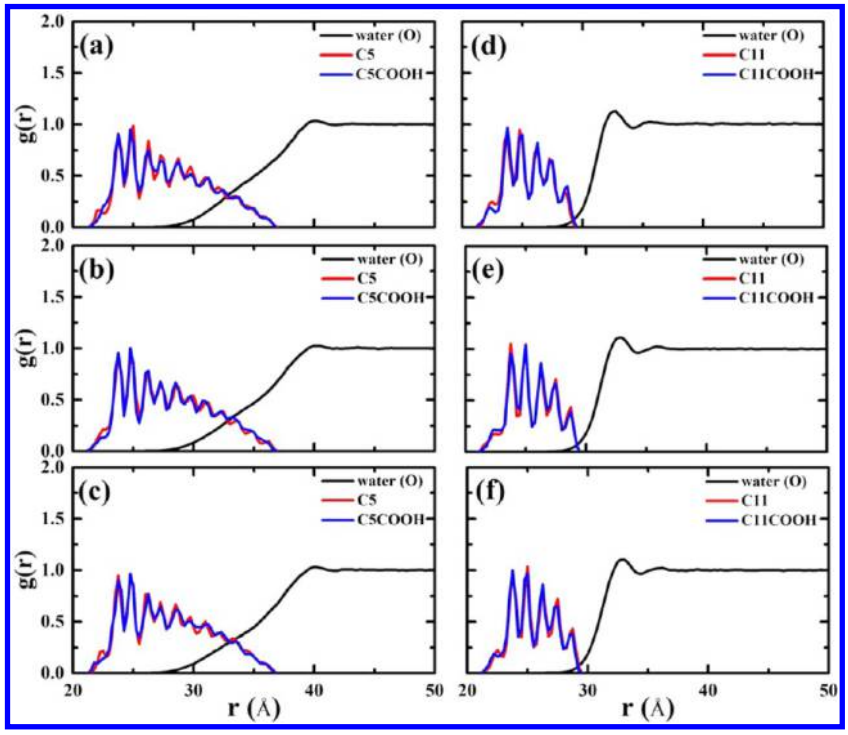

Figure 5. Radial distribution of water oxygen and carbon atoms of thiols (excluding terminal carbon atoms) from the center of AuNPs for mixing of equal carbon lengths at random [(a) and (d)], patchy [(b) and (e)] and Janus [(c) and (f)]. The left column is for C5−C5COOH SAMs, and the right one is for C11−C11COOH SAMs.

DOI: 10.1021/jp512144g
J. Phys. Chem. C 2015, 119, 3199−3209

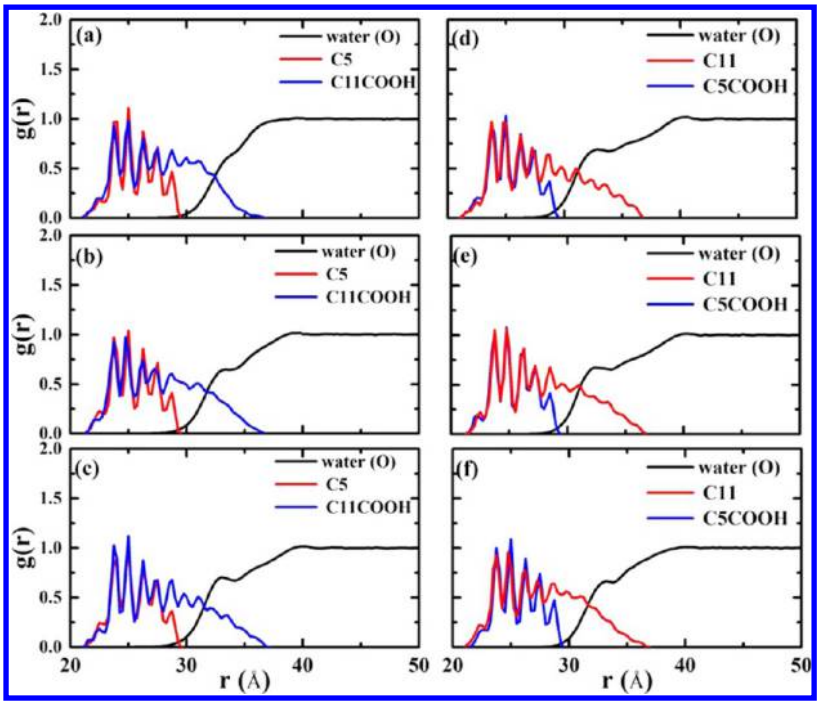

Figure 6. Radial distribution of water oxygens and carbon atoms of thiols (excluding terminal carbon atoms) from the center of AuNPs for mixing of unequal alkyl thiol lengths at random [(a) and (d)], patchy [(b) and (e)] and Janus [(c) and (f)]. The left column is for C5−C11COOH SAMs, and the right one is for C11−C5COOH SAMs.

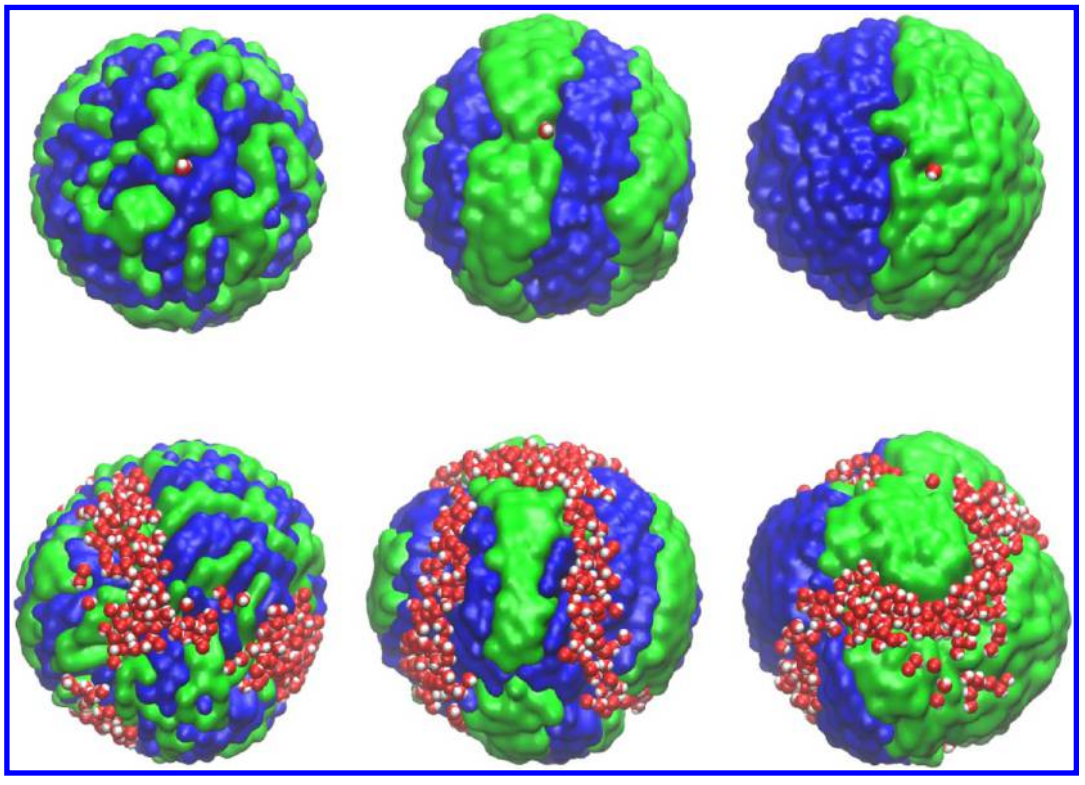

Figure 7. Snapshots taken from the simulations displaying the water molecules entering between the thiols in mixed SAMs of C5−C5COOH (top row) and C11−C11COOH (bottom row) coated on AuNPs at random, patchy, and Janus arrangements (from left to right). Color coding: methyl terminated alkanethiols, blue; carboxyl terminated alkanethiols, green; and water molecules, red (oxygen) and white (hydrogen).

arrangements yields notable different structural morphologies for the C5−C11COOH mixing and the C11−C5COOH mixing. To summarize, our results show that the bending of longer thiols depends on the thiols arrangements as well as the chemical composition of the terminal groups. The arrangements of thiols onto the AuNPs can have significant effects on their hydration behavior as it will be seen subsequently.

3.4. Radial Distribution Functions and Hydration. The radial distribution functions (RDFs) of oxygen atoms of water molecules and carbon atoms (CH_2) of the alkyl groups

DOI: 10.1021/jp512144g
J. Phys. Chem. C 2015, 119, 3199−3209

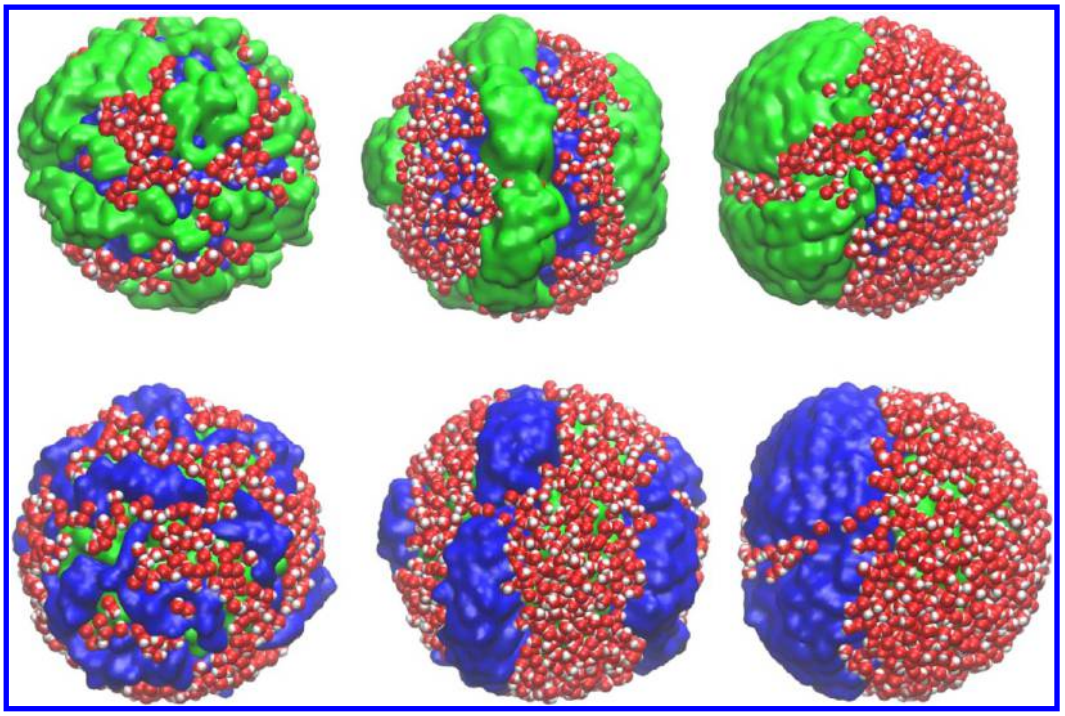

Figure 8. Snapshots taken from the simulations displaying the water molecules entering between the thiols in mixed SAMs of C5−C11COOH (top row) and C11−C5COOH (bottom row) coated on AuNPs at random, patchy and Janus arrangements (from left to right). Color-coding as in Figure 7.

Table 3. Average Number of Water Molecules in Two Particular Regions for All the Cases

	region I[a]			region II[b]		
	ran	pat	Jan	Ran	Pat	Jan
C5−C5COOH	1 ± 1	1 ± 1	1 ± 1	1052 ± 20	1037 ± 21	1024 ± 20
C11−C11COOH	489 ± 26	489 ± 20	505 ± 20	1953 ± 23	1953 ± 22	1941 ± 24
C5−C11COOH	353 ± 32	748 ± 35	978 ± 28	2223 ± 25	2353 ± 25	2416 ± 23
C11−C5COOH	687 ± 30	1213 ± 30	1102 ± 34	2287 ± 26	2428 ± 24	2365 ± 26

[a]Considering the water molecules within the radius of SAMs (excluding terminal groups). [b]Considering the water molecules from region I to region I plus 5 Å.

excluding the terminal carbon atoms (CH_3 and COOH) from the center of the AuNP can provide a microscopic picture of thiol hydration. The spatial arrangement of water and SAMs from AuNPs reveals the nature of water molecules in the vicinity of SAMs. Depending on the spatial behavior of water molecules and carbon atoms of thiols, one can conclude whether the water molecules stay near the terminal groups or enter into the SAMs. Furthermore, from this information, one can also understand whether NPs have free volume to have water molecules nearby or not. In order to study the above features, we calculated the RDFs of oxygen atoms of water molecules and the carbon atoms of thiols from the center of mass of AuNPs, which are depicted in Figures 5 and 6 for all the cases. As can be seen, in the case of lower chain lengths, the overlapping zone of the water RDF and the alkyl RDF is lower than that of longer chains. This reveals that the hydration of the SAMs is almost same for equal carbon chain length mixing but differs for unequal mixing. The RDFs of water oxygen for all types of mixing exhibit some atomic layering behavior but the profiles are markedly different among equal and unequal chain length mixing even between the C5−C5COOH and C11−C11COOH mixings. The RDFs of water oxygen for the C5−C5COOH mixing shows a noticeable two shell atomic layering behavior (Figure 5d−f). In this C5−C5COOH assembly, the RDFs of alkyl chains consist of sharp peaks pertaining to a rigid structure of the monolayer, and their negligible intersection with the RDFs of water oxygen indicates minor water penetration into the monolayer, as can be seen in Figure 7 (top row). However, in the C11−C11COOH mixing, the RDF profiles exhibit less pronounced single layer behavior (Figure 5a−c). Due to the higher available free volume, the chains are grouped together yielding then more free volume for water penetration. From Figure 7 (bottom row), it can be observed that there is layering of waters inside the monolayer in this kind of mixing.

The waters' RDFs show a very distinct behavior for the cases of mixing of thiols with unequal carbon chains. In the case of C5−C11COOH mixing (Figure 6, left column), the waters' RDFs are not overlapping with the RDFs of hydrophobic thiols, which mean that waters do not penetrate into the layer; whereas the hydrophilic thiols show intersection with the water. In the case of the random mixtures, the bending of longer chains hinders the water molecules penetration and this leads to a sharper drop in the RDFs compared to the other two cases. This hindrance for water penetration can be concluded from the appearance of a less distinct hump in the RDFs of water

DOI: 10.1021/jp512144g
J. Phys. Chem. C 2015, 119, 3199−3209

Table 4. Average Number of Water−Water Hydrogen Bonds ($N_{w\text{-}w}$) per Water Molecules at Three Different Regions for all the cases

	region I[a]			region II[b]			region III[c]		
	ran	pat	Jan	ran	Pat	Jan	ran	pat	Jan
C5−C5COOH				2.84 ± 0.03	2.82 ± 0.03	2.81 ± 0.03	3.44 ± 0.02	3.44 ± 0.02	3.44 ± 0.02
C11−C11COOH	2.94 ± 0.05	2.95 ± 0.05	2.98 ± 0.05	3.20 ± 0.02	3.19 ± 0.02	3.18 ± 0.02	3.42 ± 0.02	3.42 ± 0.02	3.42 ± 0.02
C5−C11COOH	2.70 ± 0.06	3.06 ± 0.03	2.96 ± 0.04	3.19 ± 0.02	3.30 ± 0.02	3.27 ± 0.02	3.44 ± 0.02	3.43 ± 0.02	3.44 ± 0.02
C11−C5COOH	2.66 ± 0.04	2.94 ± 0.03	2.94 ± 0.03	3.34 ± 0.02	3.38 ± 0.02	3.38 ± 0.02	3.45 ± 0.02	3.44 ± 0.02	3.44 ± 0.02

[a]Considering the water molecules within the radius of SAMs (excluding terminal groups). [b]Considering the water molecules from region I to region I plus 5 Å. [c]Considering the water molecules from region II to region II plus 5 Å.

between 30 and 35 Å. Moreover, the RDFs of water reach unity more quickly than for the two other cases. In the case of longer hydrophobic thiols, the long chains allow space for water molecules to penetrate and form strips of water molecules within the monolayer. Water molecules form layering on the top of the hydrophilic thiols, which are smaller in size. This can be easily visualized by examining Figure 8 (bottom row), which shows the arrangement of water molecules on the C11−C5COOH mixed SAMs.

To gather a quantitative measurement of the hydration of SAMs, we have calculated the number of water molecules within the radius of SAMs excluding terminal groups (say, region I) and from the above region to 5 Å (say, region II). Table 3 summarizes the number of water molecules in the two regions. In the case of C5−C11COOH and C11−C5COOH mixing, the radius of the SAMs was calculated by considering the longer thiols C11 carbon atoms. From the results in Table 3, we observe that the number of water molecules is the same for both C11−C11COOH and C5−C5COOH mixings at three different arrangements but differs for C5−C11COOH and C11−C5COOH mixings. Notice here that in contrast to our results, Kuna et al.[26] predicted that the stripped arrangement (<2 nm width) shows slightly larger hydrophilicity compared to the Janus arrangement for binary mixtures of 1-octanethiol and 6-mercaptohexan-1-ol of varying ratios. This disagreement is likely due to the difference in the hydrophilic nature of the terminal groups, the alkyl chain lengths and, most importantly, the patchy width. As the C5−C5COOH mixing has lesser free volume per chain,[29,30] leading to lower tilt angles, this allows only 1−2 water molecules between the SAMs. The snapshots shown in Figures 7 and 8 visualize the water molecules entering between the thiols for the mixed SAMs coated on AuNPs in all the cases. Interestingly, a rich response is observed for the cases of C11−C11COOH, C5−C11COOH, and C11−C5COOH mixings, with the number of water molecules between the SAMs ranging from 500 to 1215, which is a quite large number compared to that seen for the C5−C5COOH mixing. Since methyl terminal groups repel the water molecules from the surface, fewer water molecules are found near the SAMs surface for the C5−C11COOH mixing than that related to the C11−C5COOH mixing. As in the C5−C11COOH and C11−C5COOH random mixing cases, the number of water molecules entering between the SAMs is always lower compared to the other two kinds of mixing arrangements. Unlike the other two cases, here the C11 alkanethiols tilted along with bending (see Figure 4) so as to fill the free volume provided by the C5 alkanethiols. In the case of C11−C5COOH mixing, the patchy arrangement shows a lower tilt angle and hence has more free volume to accommodate more water molecules. Further, the distribution $P(R/R_0)$ also shows a slightly larger peak at R/R_0 =1 for C11−C5COOH patchy mixing. From all these observations, we conclude that the SAMs are hydrated alike for equal chain length mixing but differ for unequal carbon chain length mixing at three different arrangements.

3.5. Hydrogen Bonding. AuNPs coated with SAMs of alkanethiols of the entire cases have the same number of hydrogen bond donor and acceptor polar groups. However, the RDFs of water oxygen atoms exhibited slightly different distribution profiles at three different arrangements for unequal carbon chain length mixing. To probe the above difference quantitatively, we have calculated the water−water hydrogen bonds per water molecule at three different regions, namely at regions I and II, already described in the previous section, as well as region III defined by considering the water molecules above region II plus 5 Å. We have used the hydrogen bond criterion of Luzar and Chandler,[50] in which a hydrogen bond exists if the distance between the participating oxygen atoms is less than 3.5 Å and simultaneously the O—H···O angle is less than 30°. Table 4 shows the average number of hydrogen bonds per water molecule ($N_{w\text{-}w}$) at three different regions for all the cases. To show the similar behavior of the water RDFs profiles for equal length mixing at three different arrangements, we also calculated $N_{w\text{-}w}$ for the C5−C5COOH and C11−C11COOH mixing cases. As expected, the value of $N_{w\text{-}w}$ in region III approaches that of bulk water (3.5), and it is lower in the other two regions. The main reason for this lower $N_{w\text{-}w}$ value is the ability of the carboxyl terminal groups to form hydrogen bonds with the water molecules (see Table 5, which shows the average number of carboxyl-water hydrogen bonds ($N_{co\text{-}w}$) per carboxyl group for all the cases.). In other words, a competing effect arises between the water−water hydrogen bonding mechanism and the carboxyl-water hydrogen bonding one ($N_{CO\text{-}w}$). Hence, the probability of establishing hydrogen bonds between the water molecules is reduced. The reduction in $N_{w\text{-}w}$ varies among the AuNPs with longer carboxyl terminal thiols ($N_{w\text{-}w} \approx 3.20$) and the AuNPs with shorter carboxyl terminal thiols ($N_{w\text{-}w} \approx 2.85$). As a consequence of the free volume provided by the longer thiols, some free water molecules exist in the region where the water molecules may be affected by the carboxyl groups, and thus the value of $N_{w\text{-}w}$ is

Table 5. Average Number of Water-Carboxyl Terminal Group Hydrogen Bonds ($N_{CO\text{-}w}$) per Carboxyl Terminal Group for All the Cases

	ran	pat	Jan
C5−C5COOH	2.19 ± 0.09	2.10 ± 0.09	2.05 ± 0.09
C11−C11COOH	2.21 ± 0.08	2.14 ± 0.07	2.12 ± 0.07
C5−C11COOH	2.34 ± 0.08	2.27 ± 0.08	2.10 ± 0.07
C11−C5COOH	1.97 ± 0.07	2.07 ± 0.07	2.06 ± 0.07

DOI: 10.1021/jp512144g
J. Phys. Chem. C 2015, 119, 3199−3209

larger compared to AuNPs with shorter carboxyl thiols. In the case of C5−C5COOH and C11−C11COOH mixings, the values of $N_{w\text{-}w}$ are almost constant in all regions for the three different arrangements. However, the values of $N_{w\text{-}w}$ are not constant in region I for the case of mixing of thiols with unequal chain lengths at the three different arrangements. In the case of C5−C11COOH mixing, the longer thiols are carboxyl terminated and therefore significant variations in the $N_{w\text{-}w}$ values appear as well in region II. Particularly, for random mixing, the longer thiols are bending over shorter thiols that enforce orientational freedom for the terminal groups. The above-mentioned terminal groups freedom yields more possibility to the formation of hydrogen bonds between carboxyl and water (see Table 5). Hence, the water−water hydrogen bonds are slightly lesser for the random mixing compared to the other two kinds of mixing. Further, because of the bending, the water−water hydrogen bond gets interrupted and thereby, the random mixing of thiols with unequal carbon chain lengths exhibits a lower $N_{w\text{-}w}$ value in region I. Even though the values of $N_{w\text{-}w}$ for the C5−C5COOH and C11−C11COOH mixings are almost similar in all regions, there are some differences in the values of $N_{CO\text{-}w}$. For mixed thiols with unequal carbon chain length, the C11−C5COOH mixing shows slightly lower values of $N_{CO\text{-}w}$ compared to the C5−C11COOH one. The reason behind this is that, the shorter thiols with carboxyl terminated groups in the C5−C11COOH mixing structure enforces orientational restrictions on the carboxyl terminal groups, which in turn affects significantly the carboxyl-water hydrogen bond formation (see Table 5). Further, due to the formation of small clusters and larger clusters of thiols, one can notice a larger difference in the total number of carboxyl-carboxyl hydrogen bonds (N_{CO-CO}) values for equal carbon chain length mixing than for the unequal carbon chain length mixing as shown in Table 6. Our results

Table 6. Average Number of Hydrogen Bonds between the Carboxyl Terminal Groups of SAMs (N_{CO-CO}) for All the Cases

	ran	pat	Jan
C5−C5COOH	5 ± 1	10 ± 2	14 ± 2
C11−C11COOH	4 ± 1	9 ± 1	10 ± 2
C5−C11COOH	8 ± 2	7 ± 1	11 ± 1
C11−C5COOH	9 ± 1	10 ± 2	13 ± 2

show that, although all the NPs have the same numbers of hydrogen bond donor and acceptor of the polar groups, due to the arrangements of the thiols, both the $N_{CO\text{-}w}$ and the N_{CO-CO} vary for all kinds of mixing (Tables 5 and 6). Variation in $N_{w\text{-}w}$ for mixing of thiols with unequal carbon chain lengths is observed too. All these results suggest that the interaction with other molecules of SAMs coated onto the AuNPs will be affected by the organization of the mixed thiols.

4. CONCLUSIONS

In this work, we have investigated the structural morphology of SAMs with mixture of equal chain lengths and unequal chain lengths at three different arrangements through all-atom MD simulations. The obtained results for the tilt angles and R_g values lead us to conclude that the structural morphology of mixed SAMs on AuNPs depends on the arrangement, the carbon chain length and the chemical composition of the terminal groups of thiols. Our results on the number of water molecules in the vicinity of SAMs reveal that the hydration of mixed SAMs is almost constant for equal length of mixing but varies for unequal length mixing at three different arrangements. As a result of the bending of longer thiols over shorter thiols, less number of water molecules enters between SAMs for random mixing at unequal carbon chain length mixing of thiols. Although the number of water molecules, the overlapping area and the end-to-end distance distributions for the C11−C11COOH mixing were found to be almost identical for the three different arrangements, the organization of thiols is different for patchy mixing compared to the other two kinds of mixing.

In conclusion, the results from unequal carbon chain length mixing suggest that the thiols with either shorter or longer SAMs surface for the patchy and Janus mixing will have a better affinity toward any other foreign molecule than the random mixed thiols. We believe that the present study provides a better understanding of the structure and hydration of SAMs with equal/unequal mixed carbon chain length of thiols on AuNPs at three different arrangements. Further, the obtained end-to-end distance distributions show that the bending of longer thiols (C11) over shorter thiols (C5) exclusively depends on the arrangements of thiols and on the chemical composition of terminal groups. Particularly, it seems that the presence of small regions with ordered (1 CH_3 × 1 COOH) mixing arrangement in random mixtures leads to thiols bending and thus, another interesting question is whether or not such bending occurs in a completely ordered arrangement. Another appealing question is as follows: What is the optimum patchy width for thiols to be absorbed onto AuNPs without bending? Therefore, it would also be important to know how both the structural morphology and hydration of SAMs are affected by changing the patchy width. Similar kinds of investigations to target such issues are presently being carried out in our laboratory.

AUTHOR INFORMATION

Corresponding Authors

*E-mail: vasuphy@gmail.com.

*E-mail: ncordeir@fc.up.pt.

Notes

The authors declare no competing financial interest.

ACKNOWLEDGMENTS

This work received financial support from the European Union (FEDER funds through COMPETE) and National Funds (FCT, Fundação para a Ciência e Tecnologia) through projects PTDC/CTMNAN/112241/2009 and Pest-C/EQB/LA0006/2013. The work also received financial support from the European Union (FEDER funds) under the framework of QREN through Project NORTE-07-0124-FEDER-000067-NANOCHEMISTRY. This work was also partially supported by the Indo-Portuguese Programme of Cooperation in Science and Technology. To all financing sources, the authors are greatly indebted as well as to the HPC Centre, IIT Kanpur for computational facility.

REFERENCES

(1) Pengo, P.; Polizzi, S.; Pasquato, L.; Scrimin, P. Carboxylate-imidazole cooperativity in dipeptide-functionalized gold nanoparticles with esterase-like activity. *J. Am. Chem. Soc.* **2005**, *127*, 1616−1617.

(2) Daniel, M. C.; Astruc, D. Gold nanoparticles: Assembly, supramolecular chemistry, quantum-size-related properties, and

DOI: 10.1021/jp512144g
J. Phys. Chem. C 2015, 119, 3199−3209

applications toward biology, catalysis, and nanotechnology. *Chem. Rev.* **2004**, *104*, 293−346.
(3) Rosi, N. L.; Mirkin, C. A. Nanostructures in biodiagnostics. *Chem. Rev.* **2005**, *105*, 1547−1562.
(4) Ghosh, P.; Han, G.; De, M.; Kim, C. K.; Rotello, V. M. Gold nanoparticles in delivery applications. *Adv. Drug Delivery Rev.* **2008**, *60*, 1307−1315.
(5) De, M.; Ghosh, P. S.; Rotello, V. M. Applications of nanoparticles in biology. *Adv. Mater.* **2008**, *20*, 4225−4241.
(6) Aili, D.; Mager, M.; Roche, D.; Stevens, M. M. Hybrid nanoparticle-liposome detection of phospholipase activity. *Nano Lett.* **2011**, *11*, 1401−1405.
(7) Lucarini, M.; Franchi, P.; Pedulli, G. F.; Gentilini, C.; Polizzi, S.; Pengo, P.; Scrimin, P.; Pasquato, L. Effect of core size on the partition of organic solutes in the monolayer of water-soluble nanoparticles: An ESR investigation. *J. Am. Chem. Soc.* **2005**, *127*, 16384−16385.
(8) Childsey, C. E. D. Free energy and temperature dependence of electron transfer at the metal-electrolyte interface. *Science* **1991**, *251*, 919−922.
(9) Zhao, X.; Leng, Y.; Cummings, P. T. Self-assembly of 1,4-benzenedithiolate/tetrahydrofuran on a gold surface: A monte carlo simulation study. *Langmuir* **2006**, *22*, 4116−4124.
(10) Thomas, K. G.; Kamat, P. V. Chromophore-functionalized gold nanoparticles. *Acc. Chem. Res.* **2000**, *36*, 888−898.
(11) Shipway, A. N.; Katz, E.; Willner, I. Nanoparticle arrays on surfaces for electronic, optical, and sensor applications. *Chem.Phys.Chem.* **2000**, *1*, 18−52.
(12) Jackson, A. M.; Myerson, J. W.; Stellacci, F. Spontaneous assembly of subnanometre-ordered domains in the ligand shell of monolayer-protected nanoparticles. *Nat. Mater.* **2004**, *3*, 330−336.
(13) Jackson, A. M.; Hu, Y.; Silva, P. J.; Stellacci, F. From homoligand- to mixed-ligand-monolayer-protected metal nanoparticles: A scanning tunneling microscopy investigation. *J. Am. Chem. Soc.* **2006**, *128*, 11135−11149.
(14) Ong, Q. K.; Reguera, J.; Silva, P. J.; Moglianetti, M.; Harkness, K.; Longobardi, M.; Mali, K. S.; Renner, C.; Feyter, S. D.; Stellacci, F. High-resolution tunneling microscopy characterization of mixed monolayer protected gold nanoparticles. *ACS Nano* **2013**, *7*, 8229−8539.
(15) Centrone, A.; Hu, Y.; Jackson, A. M.; Zerbi, G.; Stellacci, F. Phase separation on mixed-monolayer-protected metal nanoparticles: A study by infrared spectroscopy and scanning tunneling microscopy. *Small* **2007**, *3*, 814−817.
(16) Lucarini, M.; Pasquato, L. ESR spectroscopy as a tool to investigate the properties of self-assembled monolayers protecting gold nanoparticles. *Nanoscale* **2010**, *2*, 668−676.
(17) Harkness, K. M.; Balinski, A.; McLean, J. A.; Cliffel, D. E. Nanoscale phase segregation of mixed thiolates on gold nanoparticles. *Angew. Chem., Int. Ed.* **2011**, *50*, 10554−10559.
(18) Wang, Y. F.; Zeiri, O.; Neyman, A.; Stellacci, F.; Weinstock, I. A. Nucleation and island growth of alkanethiolate ligand domains on gold nanoparticles. *ACS Nano* **2011**, *6*, 629−640.
(19) Bonomi, R.; Cazzolaro, A.; Prins, L. J. Assessment of the morphology of mixed SAMs on Au nanoparticles using a fluorescent probe. *Chem. Commun.* **2011**, *47*, 445−447.
(20) Liu, X.; Yu, M.; Kim, H.; Mameli, M.; Stellacci, F. Determination of monolayer-protected gold nanoparticle ligand−shell morphology using NMR. *Nat. Commun.* **2012**, *3*, 1182.
(21) Luedtke, W. D.; Landman, U. Structure, dynamics, and thermodynamics of passivated gold nanocrystallites and their assemblies. *J. Phys. Chem.* **1996**, *100*, 13323−13329.
(22) Luedtke, W. D.; Landman, U. Structure and thermodynamics of self-assembled monolayers on gold nanocrystallites. *J. Phys. Chem. B* **1998**, *102*, 6566−6572.
(23) Ghorai, P. K.; Glotzer, S. C. Molecular dynamics simulation study of self-assembled monolayers of alkanethiol surfactants on spherical gold nanoparticles. *J. Phys. Chem. C* **2007**, *111*, 15857−15862.
(24) Lane, J. M. D.; Grest, G. S. Spontaneous asymmetry of coated spherical nanoparticles in solution and at liquid-vapor interfaces. *Phys. Rev. Lett.* **2010**, *104*, 235501.
(25) Ingram, R. S.; Hostetler, M. J.; Murray, R. W. Poly-Hetero-ω-functionalized alkanethiolate-stabilized gold cluster compounds. *J. Am. Chem. Soc.* **1997**, *119*, 9175−9178.
(26) Kuna, J. J.; Voitchovsky, K.; Singh, C.; Jiang, H.; Mwenifumbo, S.; Ghorai, P. K.; Stevens, M. M.; Glotzer, S. C.; Stellacci, F. The effect of nanometre-scale structure on interfacial energy. *Nat. Mater.* **2009**, *8*, 837−842.
(27) Centrone, A.; Penzo, E.; Sharma, M.; Myerson, J. W.; Jackson, M.; Marzari, N.; Stellacci, F. The role of nanostructure in the wetting behavior of mixed-monolayer-protected metal nanoparticles. *Proc. Natl. Acad. Sci. U.S.A.* **2008**, *105*, 9886−9891.
(28) Sciortino, F.; Giacometti, A.; Pastore, G. Phase diagram of Janus particles. *Phys. Rev. Lett.* **2009**, *103*, 237801.
(29) Singh, C.; Ghorai, P. K.; Horsch, M. A.; Jackson, A. M.; Larson, R. G.; Stellacci, F.; Glotzer, S. C. Entropy-mediated patterning of surfactant-coated nanoparticles and surfaces. *Phys. Rev. Lett.* **2007**, *99*, 226106.
(30) Ghorai, P. K.; Glotzer, S. C. Atomistic simulation study of striped phase separation in mixed-ligand self-assembled monolayer coated nanoparticles. *J. Phys. Chem. C* **2010**, *114*, 19182−19187.
(31) Vasumathi, V.; Cordeiro, M. N. D. S. Molecular dynamics study of mixed alkanethiols covering a gold surface at three different arrangements. *Chem. Phys. Lett.* **2014**, *600*, 79−86.
(32) Feller, S. E.; MacKerell, A. D. An improved empirical potential energy function for molecular simulations of phospholipids. *J. Phys. Chem. B* **2000**, *104*, 7510−7515.
(33) Vieceli, J.; Ma, O. L.; Douglas, J.; Tobias, J. D. Uptake and collision dynamics of gas phase ozone at unsaturated organic interfaces. *J. Phys. Chem. A* **2004**, *108*, 5806−5814.
(34) Dubowski, Y.; Vieceli, J.; Tobias, J. D.; Gomez, A.; Lin, A.; Nizkorodov, S. A.; McIntire, T. M.; Finlayson-Pitts, B. J. Interaction of gas-phase ozone at 296 K with unsaturated self-assembled monolayers: A new look at an old system. *J. Phys. Chem. A* **2004**, *108*, 10473−10485.
(35) Szori, M.; Tobias, D. J.; Roeselová, M. Microscopic wetting of mixed self-assembled monolayers: A molecular dynamics study. *J. Phys. Chem. B* **2009**, *113*, 4161−4169.
(36) Heinz, H.; Vaia, R. A.; Farmer, B. L.; Naik, R. R. Accurate simulation of surfaces and interfaces of face-centered cubic metals using 12−6 and 9−6 Lennard-Jones potentials. *J. Phys. Chem. C* **2008**, *112*, 17281−17290.
(37) Hansen, J. P.; McDonald, I. R. *Theory of Simple Liquids*; Academic Press: London, 1986.
(38) Plimpton, S. Fast parallel algorithms for short-range molecular dynamics. *J. Comput. Phys.* **1995**, *117*, 1−19.
(39) Nose, S.; Klein, M. L. Constant pressure molecular dynamics for molecular systems. *Mol. Phys.* **1983**, *50*, 1055−1076.
(40) Parrinello, M.; Rahman, A. Polymorphic transitions in single crystals: A new molecular dynamics method. *J. Appl. Phys.* **1981**, *52*, 7182−7190.
(41) Hardy, D. J.; Stone, J. E.; Schulten, K. Multilevel summation of electrostatic potentials using graphics processing units. *Parallel Computing* **2009**, *35*, 164−177.
(42) Ryckaert, J. P.; Ciccotti, G.; Berendsen, H. J. C. Numerical integration of the cartesian equations of motion of a system with constraints: Molecular dynamics of *n*-alkanes. *J. Comput. Phys.* **1977**, *23*, 327−341.
(43) Humphrey, W.; Dalke, A.; Schulten, K. VMD - Visual molecular dynamics. *J. Mol. Graphics* **1996**, *14*, 33−38.
(44) Love, J. C.; Estroff, L. A.; Kriebel, J. K.; Nuzzo, R. G.; Whitesides, G. M. Self-assembled monolayers of thiolates on metals as a form of nanotechonolgy. *Chem. Rev.* **2005**, *105*, 1103−1169.
(45) Terrill, R. H.; Postlethwaite, T. A.; Chen, C. H.; Poon, C. D.; Terzis, A.; Chen, A.; Hutchison, J. E.; Clark, M. R.; Wignall, G. D.; Londono, J. D.; et al. Monolayers in three dimensions: NMR, SAXS,

DOI: 10.1021/jp512144g
J. Phys. Chem. C 2015, 119, 3199−3209

thermal, and electron hopping studies of alkanethiol stabilized gold clusters. *J. Am. Chem. Soc.* **1995**, *117*, 12537−12548.
(46) Porter, M. D.; Bright, T. B.; Allara, D. L.; Chidsey, C. E. D. Spontaneously organized molecular assemblies. 4. Structural characterization of n-alkyl thiol monolayers on gold by optical ellipsometry, infrared spectroscopy, and electrochemistry. *J. Am. Chem. Soc.* **1987**, *109*, 3559−3568.
(47) Nuzzo, R. G.; Dubois, L. H.; Allara, D. L. Fundamental studies of microscopic wetting on organic surfaces. 1. Formation and structural characterization of a self-consistent series of polyfunctional organic monolayers. *J. Am. Chem. Soc.* **1990**, *112*, 558−569.
(48) Vemparala, S.; Karki, B. B.; Kalia, R. K.; Nakano, A.; Vashisshta, P. Large-scale molecular dynamics simulations of alkanethiol self-assembled monolayers. *J. Chem. Phys.* **2004**, *121*, 4323−4330.
(49) Rai, B.; Malhotra, C. P.; Ayappa, K. G. Molecular dynamics simulations of self-assembled alkylthiolate monolayers on an Au(111) surface. *Langmuir* **2004**, *20*, 3138−3144.
(50) Luzar, A.; Chandler, D. Effect of environment on hydrogen bond dynamics in liquid water. *Phys. Rev. Lett.* **1996**, *76*, 928−931.

DOI: 10.1021/jp512144g
J. Phys. Chem. C 2015, 119, 3199−3209